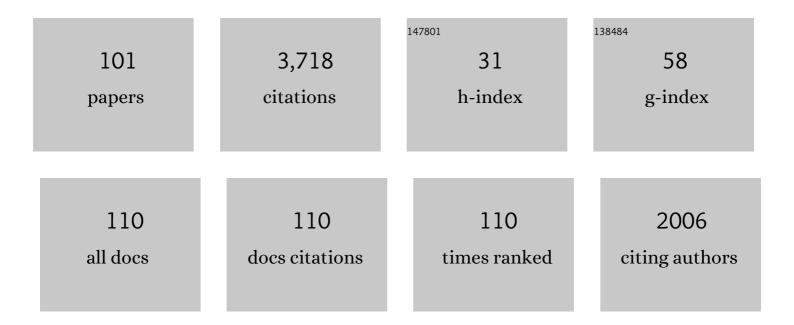
## Mauro Ciarniello

List of Publications by Year in descending order

Source: https://exaly.com/author-pdf/5983660/publications.pdf Version: 2024-02-01



#	Article	IF	CITATIONS
1	lron rich basaltic eucrites, implication on spectral properties and parental bodies. Icarus, 2022, 371, 114653.	2.5	2
2	Saturn's icy satellites investigated by Cassini - VIMS. V. Spectrophotometry. Icarus, 2022, 375, 114803.	2.5	3
3	Macro and micro structures of pebble-made cometary nuclei reconciled by seasonal evolution. Nature Astronomy, 2022, 6, 546-553.	10.1	20
4	Bayesian analysis of Juno/JIRAM's NIR observations of Europa. Icarus, 2021, 357, 114215.	2.5	7
5	Saturn System. , 2021, , 123-132.		1
6	Highâ€Temperature VISâ€IR Spectroscopy of NH <sub>4</sub> â€Phyllosilicates. Journal of Geophysical Research E: Planets, 2021, 126, e2020JE006696.	3.6	6
7	Laboratory Investigations Coupled to VIR/Dawn Observations to Quantify the Large Concentrations of Organic Matter on Ceres. Minerals (Basel, Switzerland), 2021, 11, 719.	2.0	6
8	The surface of (4) Vesta in visible light as seen by Dawn/VIR. Astronomy and Astrophysics, 2021, 653, A118.	5.1	1
9	Thermal inertia of Occator's faculae on Ceres. Planetary and Space Science, 2021, 205, 105285.	1.7	0
10	Organic Material on Ceres: Insights from Visible and Infrared Space Observations. Life, 2021, 11, 9.	2.4	12
11	VIS-IR Spectroscopy of Mixtures of Water Ice, Organic Matter, and Opaque Mineral in Support of Small Body Remote Sensing Observations. Minerals (Basel, Switzerland), 2021, 11, 1222.	2.0	4
12	VIS-NIR/SWIR Spectral Properties of H2O Ice Depending on Particle Size and Surface Temperature. Minerals (Basel, Switzerland), 2021, 11, 1328.	2.0	6
13	High Thermal Inertia Zones on Ceres From Dawn Data. Journal of Geophysical Research E: Planets, 2020, 125, e2018JE005733.	3.6	9
14	Fresh emplacement of hydrated sodium chloride on Ceres from ascending salty fluids. Nature Astronomy, 2020, 4, 786-793.	10.1	60
15	Mapping Io's Surface Composition With Juno/JIRAM. Journal of Geophysical Research E: Planets, 2020, 125, e2020JE006522.	3.6	8
16	The Philae lander reveals low-strength primitive ice inside cometary boulders. Nature, 2020, 586, 697-701.	27.8	40
17	Photometric modelling and VIS-IR albedo maps of Rhea from Cassini-VIMS. Monthly Notices of the Royal Astronomical Society: Letters, 2020, 499, L62-L66.	3.3	3
18	Infrared Observations of Ganymede From the Jovian InfraRed Auroral Mapper on Juno. Journal of Geophysical Research E: Planets, 2020, 125, e2020JE006508.	3.6	16

#	Article	IF	CITATIONS
19	A Probabilistic Approach to Determination of Ceres' Average Surface Composition From Dawn Visibleâ€Infrared Mapping Spectrometer and Gamma Ray and Neutron Detector Data. Journal of Geophysical Research E: Planets, 2020, 125, e2020JE006606.	3.6	11
20	Temporal evolution of the permanent shadowed regions at Mercury poles: applications for spectral detection of ices by SIMBIOSYS-VIHI on BepiColombo mission. Monthly Notices of the Royal Astronomical Society, 2020, 498, 1308-1318.	4.4	3
21	67P/Churyumov–Gerasimenko's dust activity from pre- to post-perihelion as detected by Rosetta/GIADA. Monthly Notices of the Royal Astronomical Society, 2020, 496, 125-137.	4.4	15
22	Ammonium salts are a reservoir of nitrogen on a cometary nucleus and possibly on some asteroids. Science, 2020, 367, .	12.6	115
23	Ceres observed at low phase angles by VIR-Dawn. Astronomy and Astrophysics, 2020, 634, A39.	5.1	8
24	Infrared detection of aliphatic organics on a cometary nucleus. Nature Astronomy, 2020, 4, 500-505.	10.1	41
25	An orbital water-ice cycle on comet 67P from colour changes. Nature, 2020, 578, 49-52.	27.8	36
26	The surface of (1) Ceres in visible light as seen by Dawn/VIR. Astronomy and Astrophysics, 2020, 642, A74.	5.1	8
27	Correction of the VIR-visible dataset from the Dawn mission at Vesta. Review of Scientific Instruments, 2020, 91, 123102.	1.3	3
28	Hydroxylated Mg-rich Amorphous Silicates: A New Component of the 3.2 μm Absorption Band of Comet 67P/Churyumov–Gerasimenko. Astrophysical Journal Letters, 2020, 897, L37.	8.3	12
29	Cassini-VIMS observations of Saturn's main rings: II. A spectrophotometric study by means of Monte Carlo ray-tracing and Hapke's theory. Icarus, 2019, 317, 242-265.	2.5	17
30	The spectral parameter maps of Ceres from NASA/DAWN VIR data. Icarus, 2019, 318, 14-21.	2.5	9
31	The mineralogy of Ceres' Nawish quadrangle. Icarus, 2019, 318, 195-204.	2.5	1
32	Analysis of night-side dust activity on comet 67P observed by VIRTIS-M: a new method to constrain the thermal inertia on the surface. Astronomy and Astrophysics, 2019, 630, A21.	5.1	8
33	Spectrophotometric modeling and mapping of Ceres. Icarus, 2019, 322, 144-167.	2.5	21
34	The changing temperature of the nucleus of comet 67P induced by morphological and seasonal effects. Nature Astronomy, 2019, 3, 649-658.	10.1	34
35	Serendipitous infrared observations of Europa by Juno/JIRAM. Icarus, 2019, 328, 1-13.	2.5	15
36	Close Cassini flybys of Saturn's ring moons Pan, Daphnis, Atlas, Pandora, and Epimetheus. Science, 2019, 364, .	12.6	24

#	Article	IF	CITATIONS
37	Comet 67P/CG Nucleus Composition and Comparison to Other Comets. Space Science Reviews, 2019, 215, 1.	8.1	32
38	VIRTIS-H observations of the dust coma of comet 67P/Churyumov-Gerasimenko: spectral properties and color temperature variability with phase and elevation. Astronomy and Astrophysics, 2019, 630, A22.	5.1	17
39	Diurnal variation of dust and gas production in comet 67P/Churyumov-Gerasimenko at the inbound equinox as seen by OSIRIS and VIRTIS-M on board Rosetta. Astronomy and Astrophysics, 2019, 630, A23.	5.1	9
40	Correction of the VIR-visible data set from the Dawn mission. Review of Scientific Instruments, 2019, 90, 123110.	1.3	9
41	Characteristics of organic matter on Ceres from VIR/Dawn high spatial resolution spectra. Monthly Notices of the Royal Astronomical Society, 2019, 482, 2407-2421.	4.4	30
42	An aqueously altered carbon-rich Ceres. Nature Astronomy, 2019, 3, 140-145.	10.1	62
43	67P/Churyumov–Gerasimenko active areas before perihelion identified by GIADA and VIRTIS data fusion. Monthly Notices of the Royal Astronomical Society, 2019, 483, 2165-2176.	4.4	8
44	Mineralogy mapping of the Ac-H-5 Fejokoo quadrangle of Ceres. Icarus, 2019, 318, 147-169.	2.5	1
45	Mineralogical analysis of the Ac-H-6 Haulani quadrangle of the dwarf planet Ceres. Icarus, 2019, 318, 170-187.	2.5	11
46	Ac-H-11 Sintana and Ac-H-12 Toharu quadrangles: Assessing the large and small scale heterogeneities of Ceres' surface. Icarus, 2019, 318, 230-240.	2.5	9
47	Mineralogical analysis of quadrangle Ac-H-10 Rongo on the dwarf planet Ceres. Icarus, 2019, 318, 212-229.	2.5	8
48	Mineralogy of the Occator quadrangle. Icarus, 2019, 318, 205-211.	2.5	11
49	Compositional differences among Bright Spots on the Ceres surface. Icarus, 2019, 320, 202-212.	2.5	33
50	Mineralogical mapping of the Kerwan quadrangle on Ceres. Icarus, 2019, 318, 188-194.	2.5	8
51	Mineralogy of the Urvara–Yalode region on Ceres. Icarus, 2019, 318, 241-250.	2.5	6
52	Photometry of Ceres and Occator faculae as inferred from VIR/Dawn data. Icarus, 2019, 320, 97-109.	2.5	17
53	Mineralogy of Occator crater on Ceres and insight into its evolution from the properties of carbonates, phyllosilicates, and chlorides. Icarus, 2019, 320, 83-96.	2.5	63
54	The surface composition of Ceres' Ezinu quadrangle analyzed by the Dawn mission. Icarus, 2019, 318, 124-146.	2.5	6

#	Article	IF	CITATIONS
55	Mineralogical mapping of Coniraya quadrangle of the dwarf planet Ceres. Icarus, 2019, 318, 99-110.	2.5	20
56	Mineralogy and temperature of crater Haulani on Ceres. Meteoritics and Planetary Science, 2018, 53, 1902-1924.	1.6	21
57	Photometric Modeling and VISâ€IR Albedo Maps of Dione From Cassiniâ€VIMS. Geophysical Research Letters, 2018, 45, 2184-2192.	4.0	7
58	Nature, formation, and distribution of carbonates on Ceres. Science Advances, 2018, 4, e1701645.	10.3	83
59	Variations in the amount of water ice on Ceres' surface suggest a seasonal water cycle. Science Advances, 2018, 4, eaao3757.	10.3	43
60	Laboratory simulations of the Vis-NIR spectra of comet 67P using sub-µm sized cosmochemical analogues. Icarus, 2018, 306, 306-318.	2.5	23
61	Continuum definition for â^¼3.1, â^¼3.4 and â^¼4.0 µm absorption bands in Ceres spectra and evaluation of effects of smoothing procedure in the retrieved spectral parameters. Advances in Space Research, 2018, 62, 2342-2354.	2.6	7
62	Ceres' opposition effect observed by the Dawn framing camera. Astronomy and Astrophysics, 2018, 620, A201.	5.1	9
63	Summer outbursts in the coma of comet 67P/Churyumov–Gerasimenko as observed by Rosetta–VIRTIS. Monthly Notices of the Royal Astronomical Society, 2018, 481, 1235-1250.	4.4	20
64	The SSDC contribution to the improvement of knowledge by means of 3D data projections of minor bodies. Advances in Space Research, 2018, 62, 2306-2316.	2.6	8
65	Ceres's global and localized mineralogical composition determined by Dawn's Visible and Infrared Spectrometer ( <scp>VIR</scp> ). Meteoritics and Planetary Science, 2018, 53, 1844-1865.	1.6	29
66	Photometric Modeling and VISâ€IR Albedo Maps of Tethys From Cassiniâ€VIMS. Geophysical Research Letters, 2018, 45, 6400-6407.	4.0	6
67	Localized aliphatic organic material on the surface of Ceres. Science, 2017, 355, 719-722.	12.6	152
68	Spectral analysis of Ahuna Mons from Dawn mission's visibleâ€infrared spectrometer. Geophysical Research Letters, 2017, 44, 97-104.	4.0	74
69	Resolved spectrophotometric properties of the Ceres surface from Dawn Framing Camera images. Icarus, 2017, 288, 201-225.	2.5	69
70	Spectrophotometric properties of dwarf planet Ceres from the VIR spectrometer on board the Dawn mission. Astronomy and Astrophysics, 2017, 598, A130.	5.1	69
71	Cometary coma dust size distribution from in situ IR spectra. Monthly Notices of the Royal Astronomical Society, 2017, 469, S598-S605.	4.4	12
72	How pristine is the interior of the comet 67P/Churyumov–Gerasimenko?. Monthly Notices of the Royal Astronomical Society, 2017, 469, S685-S694.	4.4	22

#	Article	IF	CITATIONS
73	Photometric behaviour of 67P/Churyumov–Gerasimenko and analysis of its pre-perihelion diurnal variations. Monthly Notices of the Royal Astronomical Society, 2017, 469, S346-S356.	4.4	16
74	Detection of exposed H <sub>2</sub> O ice on the nucleus of comet 67P/Churyumov-Gerasimenko. Astronomy and Astrophysics, 2016, 595, A102.	5.1	67
75	Refractory and semi-volatile organics at the surface of comet 67P/Churyumov-Gerasimenko: Insights from the VIRTIS/Rosetta imaging spectrometer. Icarus, 2016, 272, 32-47.	2.5	127
76	The global surface composition of 67P/CG nucleus by Rosetta/VIRTIS. (I) Prelanding mission phase. Icarus, 2016, 274, 334-349.	2.5	54
77	Distribution of phyllosilicates on the surface of Ceres. Science, 2016, 353, .	12.6	159
78	Seasonal exposure of carbon dioxide ice on the nucleus of comet 67P/Churyumov-Gerasimenko. Science, 2016, 354, 1563-1566.	12.6	61
79	Disk-resolved photometry of Vesta and Lutetia and comparison with other asteroids. Icarus, 2016, 267, 204-216.	2.5	11
80	Saturn's icy satellites investigated by Cassini-VIMS. IV. Daytime temperature maps. Icarus, 2016, 271, 292-313.	2.5	23
81	Bright carbonate deposits as evidence of aqueous alteration on (1) Ceres. Nature, 2016, 536, 54-57.	27.8	240
82	Exposed water ice on the nucleus of comet 67P/Churyumov–Gerasimenko. Nature, 2016, 529, 368-372.	27.8	104
83	MINERALOGICAL ANALYSIS OF THE QUADRANGLES AC-11 SINTANA AND AC-12 TOHARU ON THE DWARF PLANET CERES. , 2016, , .		1
84	MINERALOGICAL MAPPING OF THE OCCATOR QUADRANGLE. , 2016, , .		2
85	Photometric properties of comet 67P/Churyumov-Gerasimenko from VIRTIS-M onboard Rosetta. Astronomy and Astrophysics, 2015, 583, A31.	5.1	71
86	Ammoniated phyllosilicates with a likely outer Solar System origin on (1) Ceres. Nature, 2015, 528, 241-244.	27.8	276
87	The organic-rich surface of comet 67P/Churyumov-Gerasimenko as seen by VIRTIS/Rosetta. Science, 2015, 347, aaa0628.	12.6	293
88	The diurnal cycle of water ice on comet 67P/Churyumov–Gerasimenko. Nature, 2015, 525, 500-503.	27.8	199
89	Spectroscopic classification of icy satellites of Saturn II: Identification of terrain units on Rhea. Icarus, 2014, 234, 1-16.	2.5	26
90	A test of Hapke's model by means of Monte Carlo ray-tracing. Icarus, 2014, 237, 293-305.	2.5	22

#	Article	IF	CITATIONS
91	Cassini–VIMS observations of Saturn's main rings: I. Spectral properties and temperature radial profiles variability with phase angle and elevation. Icarus, 2014, 241, 45-65.	2.5	24
92	Spectral variability of plagioclase–mafic mixtures (2): Investigation of the optical constant and retrieved mineral abundance dependence on particle size distribution. Icarus, 2014, 235, 207-219.	2.5	30
93	Spectroscopic classification of icy satellites of saturn — Identification of terrain units on dione and rhea. , 2014, , .		0
94	Connections between spectra and structure in Saturn's main rings based on Cassini VIMS data. Icarus, 2013, 223, 105-130.	2.5	40
95	Spectral variability of plagioclase–mafic mixtures (1): Effects of chemistry and modal abundance in reflectance spectra of rocks and mineral mixtures. Icarus, 2013, 226, 282-298.	2.5	52
96	Spectroscopic classification of icy satellites of Saturn I: Identification of terrain units on Dione. Icarus, 2013, 226, 1331-1349.	2.5	22
97	THE RADIAL DISTRIBUTION OF WATER ICE AND CHROMOPHORES ACROSS SATURN'S SYSTEM. Astrophysical Journal, 2013, 766, 76.	4.5	26
98	Saturn's icy satellites and rings investigated by Cassini–VIMS: III – Radial compositional variability. Icarus, 2012, 220, 1064-1096.	2.5	86
99	Hapke modeling of Rhea surface properties through Cassini-VIMS spectra. Icarus, 2011, 214, 541-555.	2.5	64
100	The temporal evolution of exposed water ice-rich areas on the surface of 67P/Churyumov-Gerasimenko: spectral analysis. Monthly Notices of the Royal Astronomical Society, 0, , stw3281.	4.4	13
101	and seasonal variability. Monthly Notices of the Royal Astronomical Society, 0, , stw3177.	4.4	10